The role of recalcitrant grain boundaries in cleavage cracking in polycrystals

Y. QIAO
Department of Civil Engineering, University of Akron, Akron, OH 44325-3905, USA
E-mail: yqiao@uakron.edu

Recalcitrant grain boundaries offer an important resistance to cleavage crack advance through crack trapping. In this article, this effect is studied based on an energy analysis. It is found that the critical energy release rate is dominated by a single parameter, *Q*, that collects together factors such as work of separation, grain size, and crack length. For short cracks, the crack trapping effect leads to an increase in fracture resistance by 20–30%. For long cracks, the crack trapping effect is negligible.
© *2005 Springer Science + Business Media, Inc.*

1. Introduction

The role of grain boundaries in cleavage crack advance in polycrystals was an active research area over the years. The grain-sized microcracks in engineering metals and alloys have been noticed since post world war II years and were related to the important resistance offered by grain boundaries [1, 2]. One of the first experimental researches on this phenomenon was performed by Gell and Smith [3] on hydrogen charged Fe-3%Si alloy, through which it was concluded that the twist crystallographic misorientation was dominant. Anderson *et al*. [4] considered the fracture process of a field of hexagonal grains. In a theoretical analysis, McClintock [5] developed a ligament tearing model to take account for the extended plastic flow of grain boundaries. In this model, the fracture work associated with the fracture of the grains was ignored and the critical energy release rate G_c was taken as the total tearing work to separate the grain boundaries

$$G_c = \frac{1}{d_g^2}\left[\frac{2}{3}\frac{k_0 d_g h_1^2}{(1+2a_{c,w})}\right] \tag{1}$$

where d_g is the grain size, k_0 is the effective shear strength of the grain boundary, h_1 is the height of the ligament along the boundary that must be sheared apart to connect cleavage facets in adjacent grains, and $a_{c,w}$ is a parameter in the range of 0 to 3.6.

In a recent experimental work, Qiao and Argon [6] studied the fracture behavior of a substantial set of randomly misoriented Fe-3%Si bicrystals and quantified the relationship between the toughness of individual high-angle grain boundary and the crystal misorientation angles, based on which they discussed the cleavage cracking in a polycrystalline Fe-2%Si alloy and a decarburized 1010 steel [7]. Detailed observations of the chronology of percolation of cleavage crack front led to

a simple expression for the cleavage resistance, G_{ICPC}, of polycrystalline materials

$$\frac{G_{ICPC}}{G_{IA}} = B^* + 3.03(\Delta x_c/d_g) \tag{2}$$

where G_{IA} is the critical energy release rate of the single crystal, Δx_c is the critical penetration depth of the crack front across a high-angle grain boundary, and $B^* = 3.31$ is a material constant. In this model, both of the shear work of grain boundaries and the fracture work inside grains, as well as the work associated with the break-through process, were taken into consideration. Similar with the ligament tearing model, the cracking process was assumed to be quasi-static.

The experimental observations indicated that the cleavage front advance in polycrystals was often of a nonuniform nature [7]. The front first breaks through the grain boundaries of relatively low toughness, which will be referred to as "regular" grain boundaries in the following discussion, and then surrounds the relatively tough grain boundaries, which will be referred to as recalcitrant grain boundaries. Before the recalcitrant grain boundaries that bridge across the crack flanks are separated, they offer additional resistance through crack trapping. This effect was ignored in models introduced above and will be discussed through energy analysis in the present study.

2. Cleavage cracking across a field of grains

As discussed above, in order to study the chronology of cleavage cracking in polycrystalline materials, fracture tests in coarse-grained Fe-2%Si alloy and decarburized 1010 steel have been performed at lower shelf ductile-brittle transition region. The details of the experimental procedure were discussed elsewhere [7]. Fig. 1a shows the SEM fractography of a decarburized 1010 steel
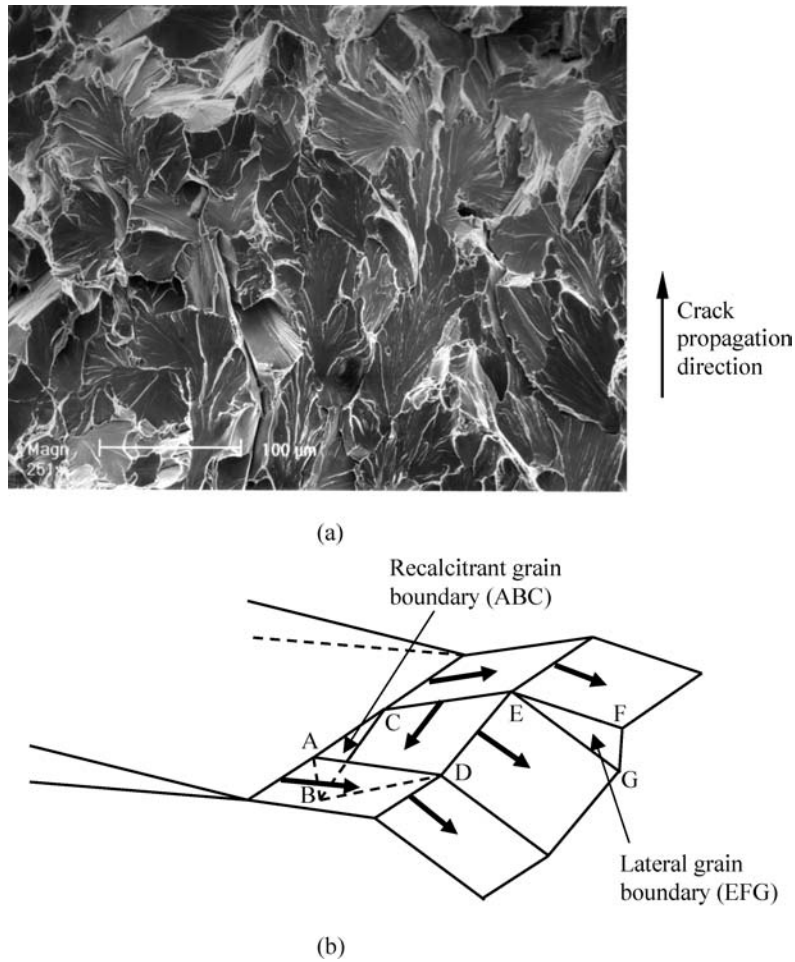
Figure 1   (a) SEM microscopy and (b) a schematic diagram of cleavage cracking across a field of grains

sample. With the complicated front profile, the crack could expose a grain either (a) at several grain boundaries simultaneously or (b) at only one boundary. If a grain boundary was too tough to be directly penetrated across, the front would break through adjacent boundaries first and the recalcitrant boundary would act as an obstacle. Eventually, the recalcitrant boundary would be sheared apart as depicted in Fig. 1b. Roughly, 10–15% of grain boundaries were of this type. Fig. 2 shows the appearance of such a grain boundary. Most of the surface shows signs of plastic shearing while there also exist evidences of fracture type separation, indicating that the boundary was separated through shear deformation combined with shear fracture under mixed-mode driving forces.

Before the recalcitrant grain boundaries are separated, the part of the cleavage front that encounters them is trapped locally, which leads to an additional fracture work associated with the crack trapping effect [8–12]. The penetration process of a crack front overcoming the resistance of a regular array of recalcitrant grain boundaries is depicted in Fig. 3. With the increasing of the overall stress intensity at the crack tip, the front starts to penetrate between the boundaries stably and, eventually when the peak resistance G_{IC} is reached, overcomes the crack trapping effect. In a polycrystalline material, the front will be arrested immediately by the next boundary array. However, since the presence of additional obstacles would not have

influence on the crack front behavior, in the following discussion we consider the case where the material ahead of line "A-A" is homogeneous. Under this condition, since G_{IC} is larger than the resistance offered by "regular" grain boundaries, the crack front will jump by a distance Δa until the energy release rate decreases to G_{IS}, the critical value to arrest the propagating crack. For reasons that will be discussed shortly, the crack jump length Δa is quite small compared with the initial crack length a_0. Thus, according to the experimental observations of dynamic cracking [13], the unstable crack advance rate is much lower than the sound speed and, consequently, G_{IS} is close to the resistance to a stationary crack, G_{I0}.

Through the fracture appearance, it is not clear whether the separation of the recalcitrant grain boundaries occurrs at the onset of the crack jump or subsequent to it. In the ligament tearing model [5], it is assumed that the boundaries are separated after the crack front has bypassed them. However, according to the numerical simulation and the experimental observation of the evolution of the profile of the cleavage front penetrating across a regular array of circular particles [9, 11], this type of front behavior cab be caused only by tough obstacles and would result in the maximum toughening effect:

$$\frac{G_{IC}}{G_{I0}} = \left(1 - \frac{w}{D}\right) + \left(2.1 + 4.8\frac{w}{D}\right)^2 \frac{w}{D} \qquad (3)$$
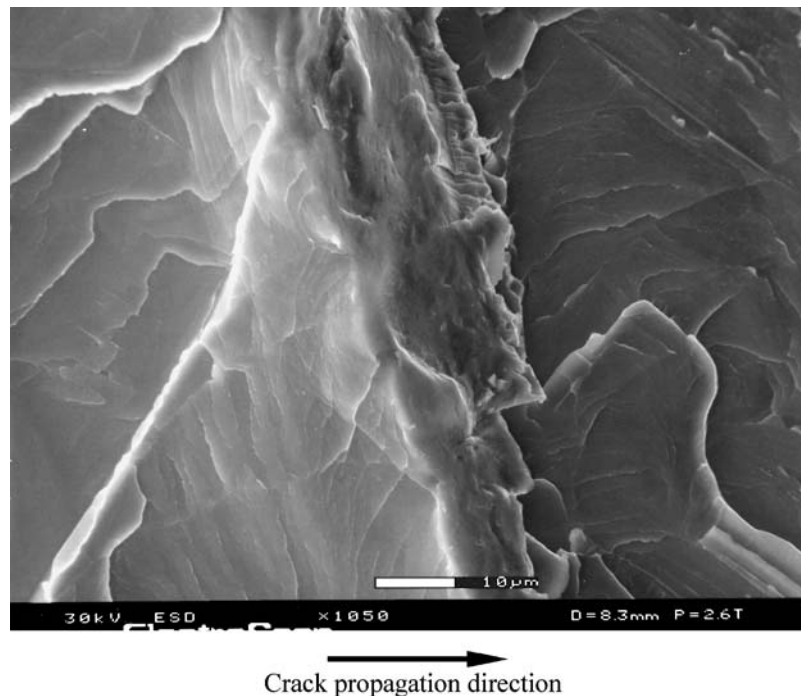
Crack propagation direction

Figure 2   A SEM micrograph of a grain boundary separated through shear deformation combined with shear fracture
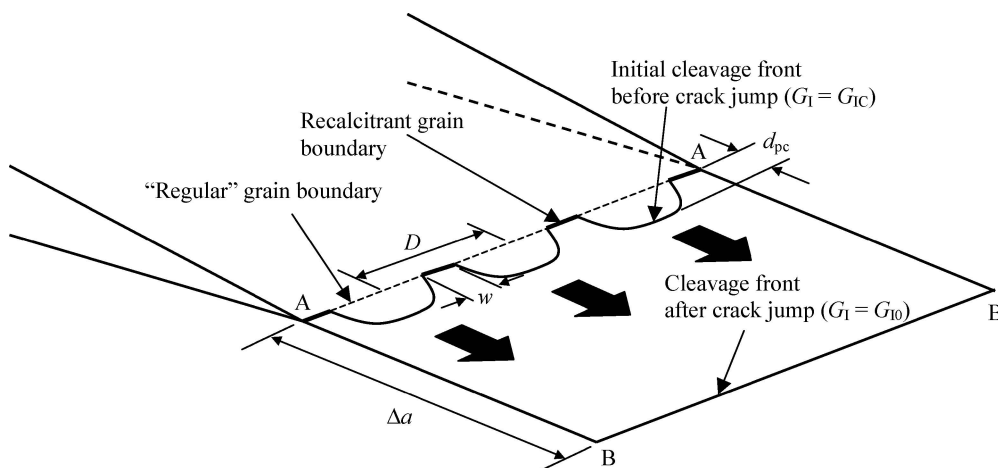

Figure 3   Cleavage cracking across a regular array of recalcitrant grain boundaries

where w and D are the width and the spacing of the obstacles, respectively. In Equation 3 if we take w/D as the line fraction of the recalcitrant grain boundaries ranging from 0.1–0.15, the G_{IC}/G_{I0} ratio is around 2.0–3.0. Even though G_{IC}/G_{I0} for grain boundaries might be slightly lower than this value, it is still too large since in Equation 2 where the crack trapping effect is ignored the calculated cleavage resistance of polycrystals is only about 3 times higher than that of the single crystal, indicating that the recalcitrant boundaries must be separated before or simultaneously when the crack starts to jump.

3. Crack trapping effect of recalcitrant grain boundaries

Based on the experimental observations discussed above, in addition to the work of separation inside grains, the overall fracture work of polycrystals consists of significant contributions from the grain bound-

aries. The first contribution is the work associated with the break-through process, and the second contribution is the work to separate the lateral grain boundaries depicted as area "EFG" in Fig. 1b. The third contribution comes from the recalcitrant grain boundaries through crack trapping. The first two contributions as well as the work of separation inside grains were taken account for in Equation 2, which, as discussed in Section 2, actually gives the resistance of "regular" boundaries.

In order to analyze the contribution of the crack trapping effect, consider cleavage cracking in the double-cantilever beam (DCB) specimen depicted in Fig. 4. The material is homogeneous with the critical energy release rate of G_{I0} offered by "regular" boundaries except for point "A", where a regular array of recalcitrant grain boundaries exist. Initially, the crack length is small and the tip is at point "D" that is far from the boundary array. With the quasi-static increasing of the crack opening displacement δ, the crack starts to grow along the median plane of the specimen. In ideal case
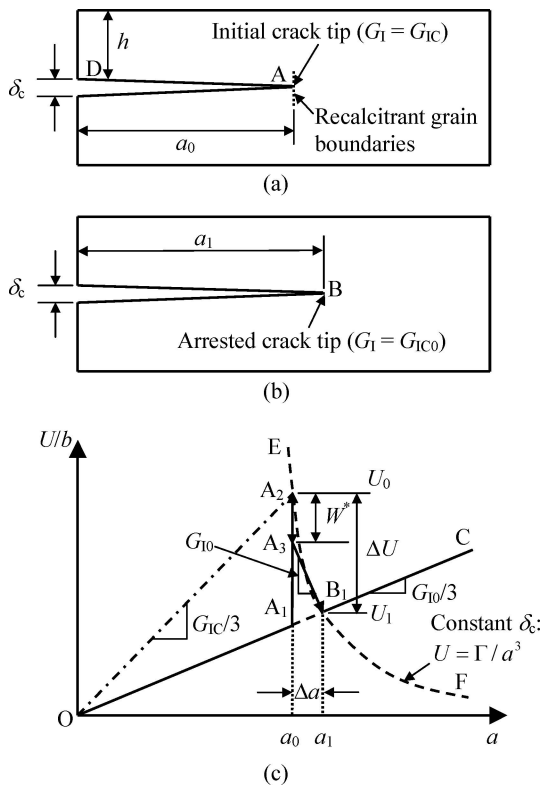
Figure 4 Crack advance in a double-cantilever beam specimen reinforced by one regular array of recalcitrant grain boundaries: (a) before the crack jump; (b) after the crack jump; (c) the relationship between the strain energy, U, and the crack length, a

where the crack tip is perfect, the crack growth is stable. The strain energy U stored in the specimen can be calculated through basic beam theory [14]. Thus,

$$\frac{U}{b} = \frac{Eh^3\delta^2}{16a^3} = \frac{a}{3}G_I \qquad (4)$$

where E is the Young's modulus, b is the specimen thickness, h is the height of the DCB arms, a is the crack length, and $G_I = -(1/b)(\partial U/\partial a)$ is the energy release rate. Since during the stable crack growth from point "D" to "A" the energy release rate G_{I0} is constant the strain energy rises linearly with the crack length a as shown by line "OA$_1$" in Fig. 4c. Once the crack front is stopped at point "A", to overcome the crack trapping effect of the recalcitrant grain boundaries the strain energy needs to be raised from "A$_1$" to "A$_2$" by increasing the crack opening displacement to δ_c until the critical condition is reached. Then the recalcitrant grain boundaries will be separated, with an energy dissipation of W^* ("A$_2$" to "A$_3$") and the crack will jump by a distance Δa from point "A" to "B", with an energy dissipation of $G_{I0}\Delta a$ ("A$_3$" to "B$_1$"), after which, with further increasing of δ, the crack advance becomes stable again and the strain energy rises along line "B$_1$C". Note that according to Equation 4 , points "O", "A$_1$", "B$_1$" and "C" are aligned in the same line with the slope of $G_{I0}/3$. During the crack jump, the crack opening displacement δ_c can be assumed to be constant, thus points "A$_2$" corresponding to the critical condition triggering the crack advance across the boundary array and "B$_1$" corresponding to the critical condition

to arrest the propagating crack are on the same curve "EF" defined by $U = \Gamma/a^3$, with $\Gamma = Eh^3\delta_c^2/16$.

At point "A$_2$", the first derivative of U does not exist. Therefore, the ordinary definition of energy release rate cannot be applied, which is in consistent with the fact that to determine the cleavage resistance caused by the crack trapping effect, not only Equation 4 but also the behavior of the recalcitrant grain boundaries must be taken account for. Nevertheless, an effective energy release rate G_{IC} can be defined based on the slope of line "OA$_2$",

$$G_{IC} = \frac{3}{16}\frac{Eh^3}{a_0^4}\delta_c^2 \qquad (5)$$

where a_0 is the crack length just before the crack jump.

When the crack is arrested at point "B",

$$G_{I0} = -\frac{\partial U}{\partial a} = \frac{3}{16}\frac{Eh^3}{a_1^4}\delta_c^2 \qquad (6)$$

where $a_1 = a_0 + \Delta a$. Through Equations 5 and 6, it can be obtained that

$$\frac{a_1}{a_0} = 1 + \frac{\Delta a}{a_0} = \tilde{G}^{1/4} \qquad (7)$$

where $\tilde{G} = G_{IC}/G_{I0}$.

The strain energy change associated with the crack jump is

$$\Delta U = U_1 - U_0 = \frac{Ebh^3\delta_c^2}{16}\left[\frac{1}{a_0^3} - \frac{1}{a_1^3}\right] \qquad (8)$$

where U_0 and U_1 are the values of the strain energy before and after the crack jump, respectively. Substitution of Equations 5 and 7 into 8 gives

$$\frac{\Delta U}{bG_{I0}} = \frac{a_0}{3}[1 - \tilde{G}^{-3/4}]\tilde{G} \qquad (9)$$

During the crack jump, the fracture work W_d consists of the work of shearing of the recalcitrant grain boundaries and the work of separation of primary fracture surfaces,

$$W_d = b \cdot W^* + G_{I0} \cdot \Delta a \cdot b \qquad (10)$$

where W^* is the effective work of separation of recalcitrant grain boundaries per unit width. If the tearing process is assumed to be pure shear combined with shear fracture as depicted in Fig. 5, W^* can be calculated as [5]

$$W^* = \frac{1}{D} \cdot \left[\frac{1}{6}\frac{kwh_0^2}{(1 + 2a_{c,w})}\right] \qquad (11)$$

where w, D, k, and h_0 are the width, the spacing, the effective shear strength, and the height of the recalcitrant grain boundary, respectively; and $a_{c,w}$ is the length of
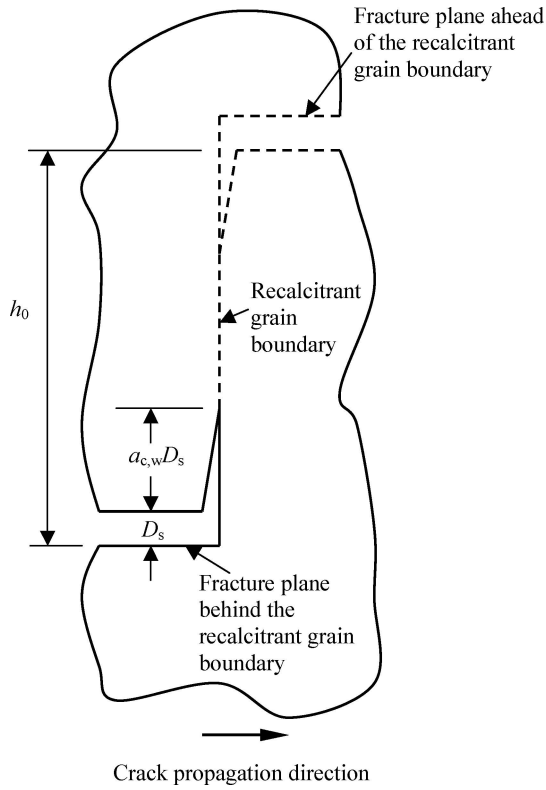
Figure 5 Ligament tearing model of the separation of recalcitrant grain boundary. The compression-side crack length is $a_{c,w}D_s$, with D_s being the shear displacement

the intergranular crack associated with unit shear distance. The value of $a_{c,w}$ is in the range of 0–3.6 [5].

Finally, since $\Delta U = W_d$, through Equations 7, 9, and 10 it can be obtained that

$$\tilde{G} - 4\tilde{G}^{1/4} = S^* \qquad (12)$$

where $S^* = Q - 3$ is a constant of the specimen, with

$$Q = \frac{1}{6a_0 D} \frac{kwh_0^2}{(1 + 2a_{c,w})G_{I0}}. \qquad (13)$$
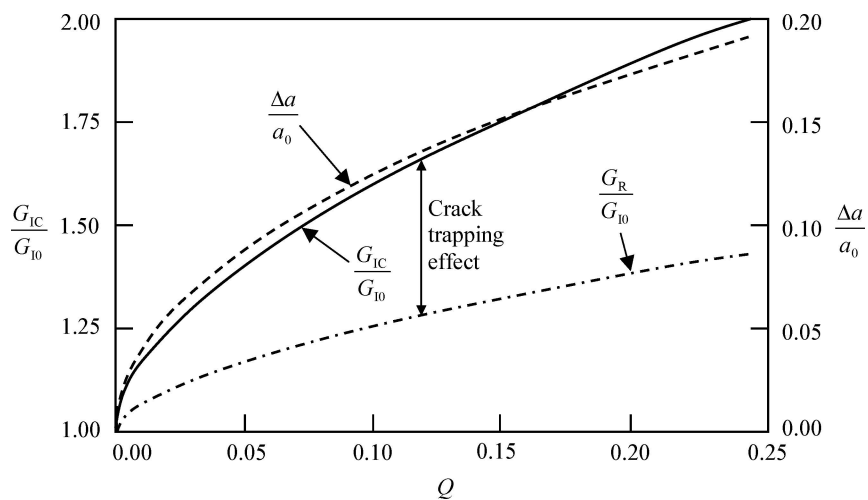
Fig. 6 shows the numerical solution of Equation 12.

4. Discussion

If we ignore the crack trapping effect, the critical energy release rate G_R to overcome an array of tough obstacles could be simply estimated as

$$G_R = G_O A_O + G_m A_m \qquad (14)$$

where G_O, G_m, A_O, and A_m are fracture resistances and area fractions of the obstacles and the matrix, respectively. For the recalcitrant grain boundaries,

$$G_R = \frac{W_d}{\Delta a \cdot b} = \frac{\Delta U}{\Delta a \cdot b} \qquad (15)$$

Substitution of Equations 7 and 9 into 15 gives

$$\frac{G_R}{G_{I0}} = \frac{1}{3} \frac{\tilde{G} - \tilde{G}^{1/4}}{\tilde{G}^{1/4} - 1} \qquad (16)$$

The comparison of G_{IC} and G_R is shown in Fig. 6. It can be seen that G_{IC} is much larger than G_R and the crack trapping effect becomes more pronounced at higher Q. When Q is in the range of 0.05 to 0.25, about 20–30% of G_{IC} is caused by crack trapping.

As discussed above, for recalcitrant grain boundaries w/D can be taken as 0.1–0.15. If the crystallographic orientation is random, $h_0/w = 0.32$ [5]. Thus, Q can be rewritten as

$$Q = \alpha \frac{kw}{(1 + 2a_{c,w}) G_{I0}} \frac{w}{a_0} \qquad (17)$$

with α being a coefficient in the range of 0.005–0.0075. If we take k as 200 MPa, G_{I0} as 730 J/m, a_0 as 100 mm, and w as 5 mm, as measured in a coarse-grained Fe-2%Si sample [7], Q is in the range of 0.04 to 0.5. Correspondingly, the value of $\tilde{G}$ is in the range of 1.3 to 2.6. Since the measured critical energy release of the polycrystalline material give only about 3-fold rise over the single crystal, and the lateral grain boundaries should have a significant contribution to the overall fracture work, the low end of this range seems more plausible, suggesting that the value of $a_{c,w}$ should be taken as

Figure 6 The critical energy release rate, G_{IC}, and the crack jump length, Δa

about 3.6. This is compatible with the observation that the fracture appearance of the boundaries consists of features of both shear deformation and fracture-type separation. The value of $\tilde{G}$ around 1.3 is considerably lower than the range of 2.0–3.0 given by Equation 2, where the recalcitrant grain boundaries were assumed to be tough and could bridge across the crack flanks even after the crack front bypassed them. The effective boundary shear strength k is dominant to the maximum penetration depth of the crack front, which in turn influences the toughening effect. With the value of $\tilde{G}$ around 1.3, through Equation 7, $\Delta a/a_0 \approx 6.7\%$, that is, the crack jump length is much smaller than the initial crack length, indicating that the above analysis is self-compatible.

For the decarburized 1010 steel samples tested at low temperatures by Qiao and Argon [7], k is around 300 MPa and w is around 50 μm. The value of G_{I0} at the lower shelf of ductile-brittle transition region was not measured but it is reasonable to assume that it is close to that of the Fe-2%Si alloy. Due to the quasi-static nature of the loading condition and the fact that the plastic deformation should be more important at the 50 μm scale, the value of $a_{c,w}$ is likely to be smaller than the peak value. As the first order approximation, we take $a_{c,w}$ as 0. Thus, Q can be estimated as $Q = 0.15(w/a_0)$. For a crack with the size of 0.5 mm, the value of Q is 0.015 and the corresponding $\tilde{G}$ is 1.22. Note that since for short cracks the line fraction of the recalcitrant grain boundaries w/D is higher, this estimate is somewhat conservative. With the increasing of the crack length, the value of $\tilde{G}$ decreases considerably. When a_0 is 5 mm, $\tilde{G}$ is 1.07; when a_0 is 50 mm, $\tilde{G}$ is 1.02. If the crack is even longer, the crack trapping effect becomes negligible. It can be seen that by considering the crack trapping effect of the recalcitrant grain boundaries the critical energy release rate of polycrystals is no longer a material constant. This should be attributed to that, with the fixed grain size, the crack growth is not self-similar. At the tip of a longer crack, the width of the recalcitrant grain boundaries seems "smaller" and consequently the toughening effect is less pronounced. Actually, through Equation 17, if the w/a_0 ratio is kept constant Q and $\tilde{G}$ become crack length independent.

This size effect can also be analyzed through Fig. 4c. With a larger crack length, the value of W^* ("A_2A_3") is still the same while the curve "EF" becomes "flatter", i.e. the crack jump length Δa tends to increase, which "dilutes" the significance of the work of separation of the recalcitrant grain boundaries. Thus, although the absolute value of the additional work required to overcome the crack trapping effect ("A_1A_2") can be higher, the slope of line "OA_2", which is one third of the effective critical energy release rate, is lowered. Note that the "flatness" of curve "EF" actually reflects the rate of change of the energy release rate, which indicates that for cleavage cracking in heterogeneous materials where the crack trapping effect is significant the critical condition of crack advance is dominated not only by the first derivative of strain energy G_I, but also by the second derivative $\partial^2 U/\partial a^2$. This phenomenon is quite similar with the crack length dependence in the well-known R-curve analysis, while in this model the fracture mode is cleavage and the cracking resistance of the matrix is constant.

Through Equation 17, it also can be seen that the value of $\tilde{G}$ is strongly dependent of grain size w. The factor of the grain size comes in by affecting both the w/a_0 ratio and the kw/G_{I0} ratio. Thus, even if w/a_0 were constant, the values of Q and $\tilde{G}$ would still be grain size dependent. This intrinsic grain size effect is caused by that the work of separation of the recalcitrant grain boundaries is proportional to w^2.

5. Conclusions

When a cleavage crack propagates across a field of grains, the front would be trapped locally at the relatively tough recalcitrant grain boundaries. This crack trapping effect results in an additional resistance to cleavage cracking. In this article, the contribution of this effect to the critical energy release rate of polycrystals is discussed, and the following conclusions are drawn:

1. The crack trapping effect of the recalcitrant grain boundaries can lead to a rise of about 20–30% of the critical energy release rate of polycrystals, which can be determined by a single parameter Q.

2. The recalcitrant grain boundaries are separated by combined shear deformation and "cleavage-like" fracture before the crack front fully bypasses them.

3. The crack trapping effect is more pronounced for shorter cracks. When the crack length is more than 100 times larger than the grain size, the crack trapping effect is negligible.

4. With a smaller grain size, the crack trapping effect becomes less significant.

References

1. N. J. PETCH, in "Progress in Metal Physics", edited by B. Chalmers and R. King (Pergamon Press, London, 1954) p. 1.
2. G. T. HAHN, B. L. AVERBACH, W. S. OWEN and M. COHEN, in Proceedings of the International Conference of Atomic Mechanisms of Fracture, Swampscott, MA (MIT Press, Cambridge, MA, 1959) p. 91.
3. M. GELL and E. SMITH, *Acta Metall.* **15** (1967) 253.
4. T. L. ANDERSON, D. STIENSTRA and R. H. DODDS, in "Fracture mechanics" Vol. 24, ASTM-STP 1207, edited by J.D. Landes et al. (ASTM, Philadelphia, NJ, 1994) p. 186.
5. F. A. MCCLINTOCK, in George R. Irwin Symposium on Cleavage Fracture, Indianapolis, IN, Sept. 1997, edited by K. S. Chan (TMS, 1997) p. 81.
6. Y. QIAO and A.S. ARGON, *Mech. Mater.* **35** (2003) 313.
7. Idem., *ibid.,* **35** (2003) 129.
8. H. GAO and J. R. RICE, *J. Appl. Mech.* **56** (1989) 828.

9. A. F. BOWER and M. ORTIZ, *J. Mech. Phys. Solids* **39** (1991) 815.

10. A. F. BOWER and M. ORTIZ, *J. Appl. Mech.* **60** (1993) 175.

11. T. M. MOWER and A. S. ARGON, *Mech. Mater.* **19** (1995) 343.

12. G. XU, A. F. BOWER and M. ORTIZ, *J. Mech. Phys. Solids* **46** (1998) 1815.

13. M. H. ALIABADI, "Dynamic Fracture Mechanics" (WIT Press, Southampton, UK, 1995).

14. O. T. BRUHNS, "Advanced Mechanics of Solids" (Springer-Verlag, NY, 2002).